OXFORD JOURNAL
OF STUDENT
SCHOLARSHIP

A Comparative Analysis of Systems for Single-Tile Chess Piece Capture Mechanisms

Atilla Aras Baysal
atillaarasbaysal@gmail.com

ABSTRACT

This research addresses the inefficiency of capture moves in automated chess, where current systems typically use the same mechanism for both standard movement and piece capture, resulting in significantly increased time, energy, and calculation. This study aims to offer a faster alternative by presenting and analysing two novel, capture-dedicated mechanisms designed to be integrated into existing automated boards. The proposed systems are designed to fit under each tile and function as a trapdoor, opening to allow a captured piece to fall into the chessboard's interior while a separate mechanism moves the capturing piece. Two designs were developed: the coupler-tile and the follower-tile model. They both utilize a combination of four-bar linkages and cam & follower systems to achieve a controlled lift and tilt. The 3D CAD models were created in Autodesk's Fusion v.2604. They were simulated and analysed using Rigid Body Dynamics simulations in ANSYS to evaluate displacement, velocity, acceleration, and joint forces over a 3-second motion. The quantitative analysis confirmed that both designs achieved the intended smooth, non-colliding motion. The follower-tile design was found to be simpler and offer greater mobility, whereas the coupler-tile design, being more complex, showed lower overall forces on its joints, suggesting improved longevity. Both mechanisms successfully demonstrate a capture time significantly faster than current automated methods, proving the viability of dedicated capture systems.

INTRODUCTION

The automation of chess presents an engineering challenge that bridges the gap between digital and on-board gameplay, compelling researchers to try and balance many aspects such as motion planning and precision mechanics. This unique topic, while seemingly straightforward, requires the consideration of many constraints, and thus, it has been a point of interest of researchers for many years, starting from the infamous "Turk". Such a creation not only adds to the intellectual entertainment sought by chess hobbyists, but can also be the sole way of enjoying this refined game for physically impaired individuals.

Papers on this subject typically discuss two methods. One method uses a robotic arm that fixes on pieces via either a magnet or a clamping mechanism. Servo motors on the multiple joints of said arms make for a system that has a very high degree of freedom. In turn, the great number of possibilities of moves slows the calculation speed while also increasing cost and fragility. For example, Ómarsdóttir et al. [1]

developed a robotic arm that uses magnets to attach to chess pieces, placing captured pieces into a separate "graveyard" bin. Similarly, Truong Duc Phuc et al. [2] designed an autonomous chess robot that relies on computer vision and deep learning to perform moves. In their system, a simple move takes about 20 seconds, a capture move about 60 seconds, and a pawn promotion roughly 90 seconds, as the robot must pick up the captured piece, place it in the storage box, and then retrieve and position the desired piece. These studies illustrate how the complexity of robotic arms leads to slower moves, higher energy expenditure, and increased fragility, echoing the limitations observed in multi-joint servo systems.

The other common method of piece movement discussed in the literature is the use of magnetic slider mechanisms placed under the board. These mechanisms lift and connect to the piece, slide it to the desired location, and lower down to disconnect. Jariyavajee et al.'s [3] interactive chess board moves captured pieces to a "killed" area located on either side of the board, while Sarker et al.'s Wizard Chess [4] system uses reed switches under the squares of removed pieces to communicate with the controller board. This method offers relative simplicity, accelerating calculation speed and reducing mechanical stress, though it lacks the multi-dimensional flexibility of a robotic arm.

To implement the precise movements such as those required in piece capture, various mechanisms have been explored in other domains of engineering. Applying these insights can help optimize robotic or slider-based chess systems by balancing flexibility, robustness, and computational efficiency. A 4-bar linkage system offers a high degree of variability, robustness, and computational simplicity. Kashef et al. [5] proposed a robot hand structure using a four-bar linkage mechanism to improve durability and motion accuracy over cable-driven designs, while Truong et al. [6] demonstrated that four-bar mechanisms can amplify flapping angles in compliant actuators. On the other hand, a cam & follower system offers superior manoeuvrability along a single axis. Mali et al. [7] highlighted its widespread application in internal combustion engines and other automated machinery, and Prasad et al. [8] analysed how cam-follower mechanisms can reduce jerk and induced stresses. These examples from broader engineering illustrate the trade-offs between multi-axis flexibility, robustness, and computational ease, providing insight into which mechanisms could optimize automated chess movement.

Yet, the automation research done on chess has never focused on diversifying capture methods, utilizing the same mechanism for both moving and capturing the pieces. Therefore, the possible applications of these mechanisms in this context were never explored. This causes the capture moves to take significantly more time than others, requiring double the amount of energy, calculations, and time. This research aims to offer an alternative to this suboptimal approach by presenting two new ways that can be integrated into existing methods.

METHODS

3.1 Design Description

This study aims to explore the aforementioned lack of capture-dedicated mechanisms on an automated chessboard. The discussed mechanisms would be inserted under each tile. These mechanisms would open,

similar to a trapdoor, and let the piece above it to fall into the chessboard itself. This would enable the capture to occur whilst another mechanism, such as a robotic arm, would move the capturing piece to the designated location.

This study therefore examines two mechanisms combining four-bar linkages with cam & follower systems to achieve the controlled lifting and tilting of a single chess tile. The envisioned systems for this tile manipulation needed to be capable of both a rising motion and slanting capabilities. A model simple enough to fit under the board and solely constituting 4-bar linkages was therefore inadequate, as the tile was unable to tilt without colliding with adjacent tiles that were level with it in the initial position. Similarly, a compact model utilizing only cam and follower systems lacked the manoeuvrability, as it could tilt the tile but not while creating an opening for the piece to fall into. Therefore, the final designs combine the range of motion that a 4-bar linkage offers with the precise lift of a cam system. The dimensions of the chess tile were chosen accordingly, measuring 40 mm on each side, to allow for easy integration of the mechanical parts. The 3D CAD designs were all made in the Autodesk's Fusion v.2604 program.

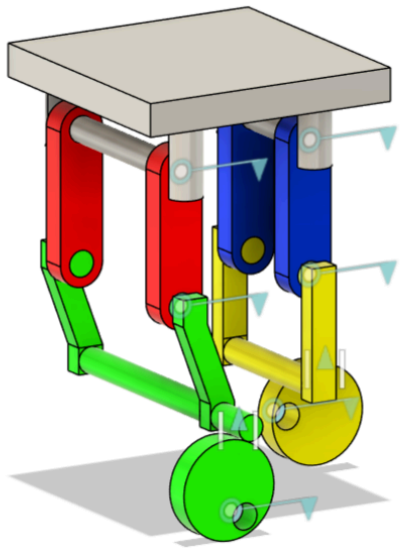

Figure 1

In *Figure 1*, the coupler-tile design is shown. This design consists of two drivers, coloured red, one coupler, coloured grey, two followers, coloured blue, one driver and one follower frame, green and yellow respectively, and one driver and one follower cam, having the same colours as their frames. It is worth mentioning that the design is simplified for demonstration and simulation purposes, omitting the guiderails for the frames' motion and the linkages of the cams to the ground. It also places handles on the cam bases for better visualization, and positions the driver cam closer to the screen. In order to have a vertical motion for the frames, translational joints that bear no load and solely determine the direction were defined for them. These changes were made in consideration of the analysis aspect, having no effect

on the data gathered. The modelling choices were made for the following reasons: The drivers were placed further apart than the followers, allowing them to tilt without collision between machine parts and to avoid the falling piece owing to the gap. The shape of the driver frame was chosen as such because having a base further than the opening of the tile allowed the chess piece to avoid impacting and getting stuck on the mechanisms.

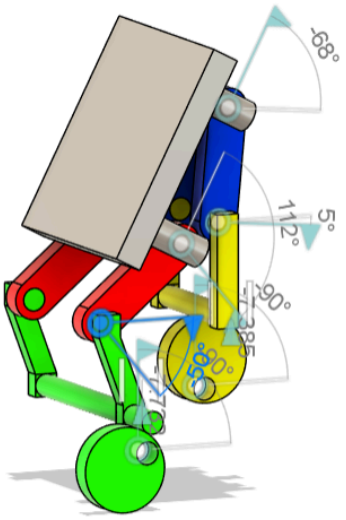

Figure 2

The motion of this design resulting in *Figure 2*, the opening of the tile, is driven by three joints. The follower frame is raised by its cam, allowing the tilt to occur without colliding with the adjacent tiles. Meanwhile, the driver frame is lowered by its cam, increasing the possible tilt by a great amount along with the follower cam. The driver, leaning towards the follower, completes the tilt.

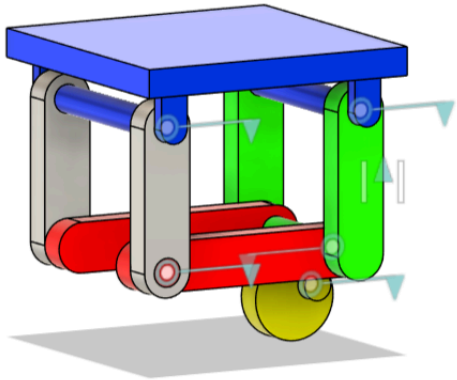

Figure 3

In *Figure 3*, the follower-tile design is shown, containing two drivers in red, two couplers in grey, a follower in blue, two frames in green, and a cam in yellow. The omissions of guiderails and cam support were also made here for the same purposes after concluding that no quantitative data would be lost. Additionally, a translational joint was added to the frame for the same purposes in the coupler-tile design. The difference between the 1.6 cm of distance between the drivers and 2.4 cm for that of the couplers allow the design to fold onto itself without collisions, creating room for the tilt.

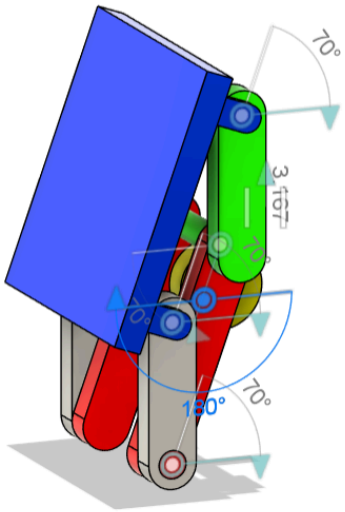

Figure 4

Possessing one fewer cam, this model is driven by two joints and resulting opening of the tile is shown in *Figure 4*. The cam raises the frame, removing the possibility of a collision between tiles, and the

driver-frame joint tilts the driver downwards, finishing the capture. The absence of a second cam lessens the complexity but puts more load on the driver-coupler and driver frame joints.

Overall, both systems were designed with the intention of producing a smooth lift and tilt. A symmetric and circular cam profile was chosen for this purpose. The equal lengths of drivers and followers and couplers and frames avoid load imbalance and result in a predictable behaviour that can be further modified.

Summary of Designs

	Coupler-tile Design *(Figure 1)*	Follower-tile Design *(Figure 2)*
Drivers	2, red	2, red
Couplers	1, the tile, grey	2, grey
Followers	2, blue	1, the tile, blue
Frames	1 driver frame, green; 1 follower frame, yellow	2 frames, connected by a cylindrical rod, green
Cams	1 driver cam, green; 1 follower cam, yellow	1, yellow
Joints	2 driver-coupler joints, 2 coupler-follower joints, 2 driver-(driver) frame joints, 2 follower-(follower) frame joints, 1 driver cam joint, 1 follower cam joint	2 driver-coupler joints, 2 coupler-follower joints, 2 driver-frame joints, 2 follower-frame joints, 1 cam joint

3.2 Simulation Setup

The models were exported from Autodesk's Fusion v.2604 to ANSYS 2025 R2 as SAT files. This change was made to make use of the Rigid Body Dynamics module of the program, offering detailed analysis of the movements and forces.

Joints were redefined, and joint loads were set for the motion-driving articulations. The coupler-tile design's cams were defined to have a rotational velocity of 30°/s, finishing their motion in 3 seconds as planned. This speed is higher than that of other automated chess captures. This duration was determined to imitate a piece capture move in a real-life chess match. The calculated 50° of tilt that the driver-frame joint was designed to have was also spread to these three seconds, resulting in the rotational speed of 16.67°/s on the driver.

The follower-tile model's driver frame joint was intended to have a rotation of 75°, and its cam was set to have a rotation of 180°. To have comparable results, the same 3 second limit was applied on this design, resulting in the rotational velocities of 25°/s for the driver frame joint and 60°/s for the cam.

The simulations measured the tile's displacement, velocity and acceleration at a sampling rate of at its centre of mass at the edge of the tile that tilts open. Joint forces, magnitudes of the X, Y and Z components, were also collected to evaluate the mechanism's efficiency, motion smoothness, and structural reliability.

The obtained graphs were exported to Microsoft Excel for processing and plotting.

3.3 Quantitative Analysis

Plots generated were as follows:

a) Positions

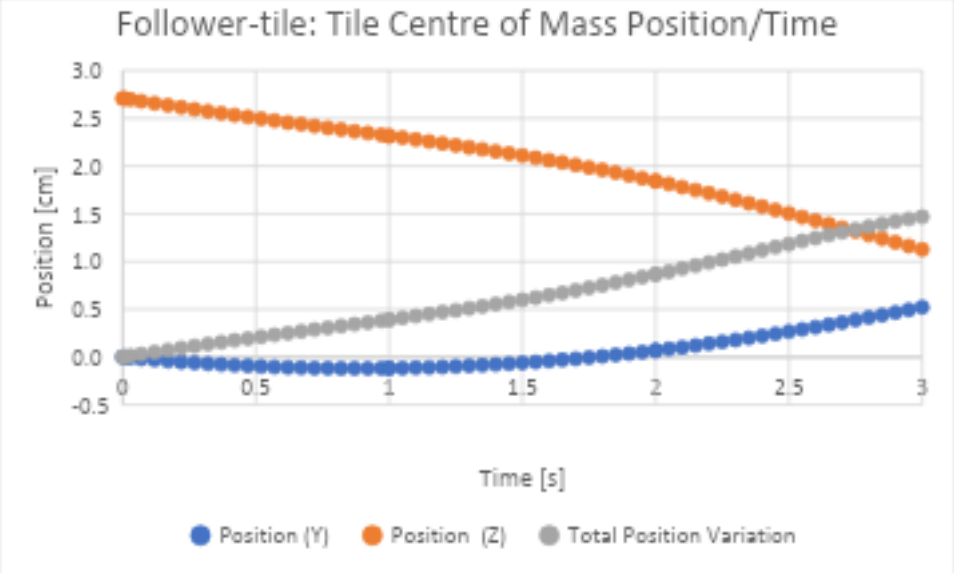

Figure 5

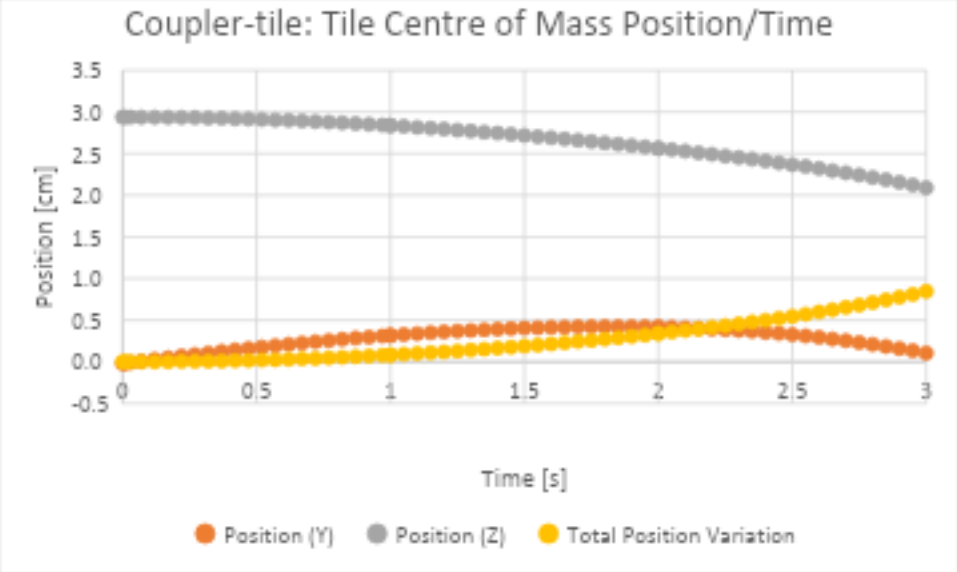

Figure 6

The graphs of positional variations of both centres of inertia are smooth curves, both reaching the maximum displacement when the tile is in its fully tilted position. The final total displacement of the follower-tile's centre of mass is approximately 1.5 cm *(Figure 5)*, while that of the coupler-tile is under 1 cm *(Figure 6)*.

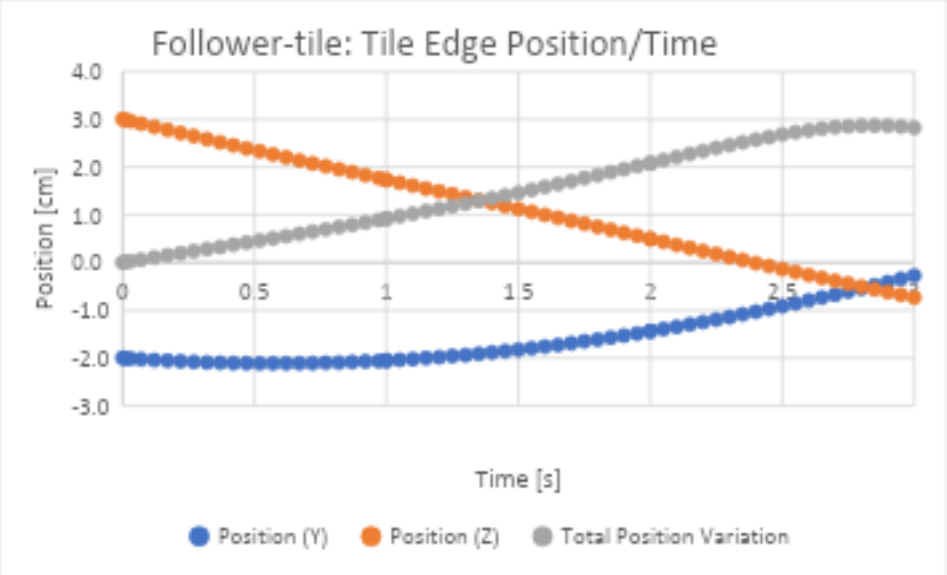

Figure 7

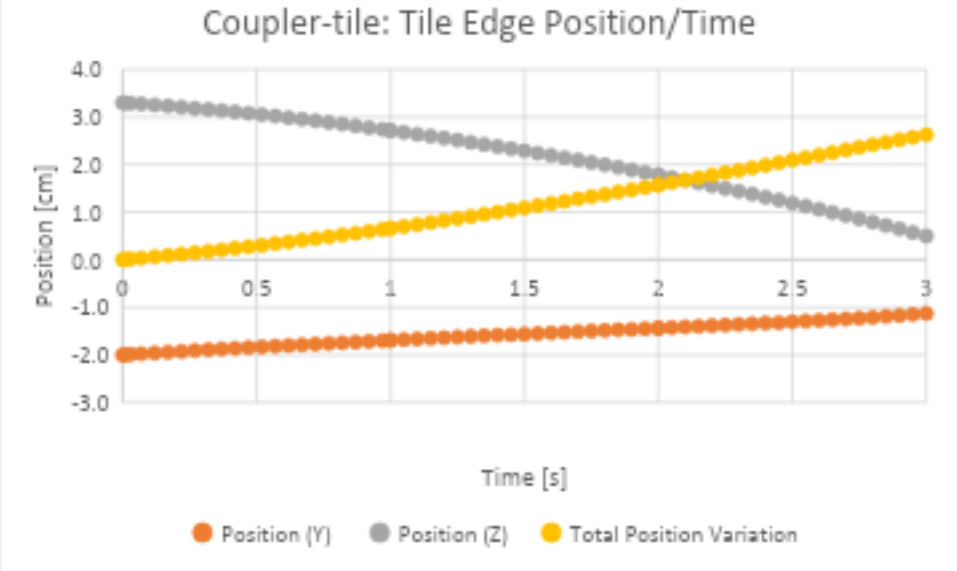

Figure 8

This trend holds true for the edge of the tile that opens as well *(Figures 7 and 8)*, and it is worth noting that the largest displacement happened on the Z axis for the follower-tile edge with almost 4 cm *(Figure 7)*.

b) Velocity

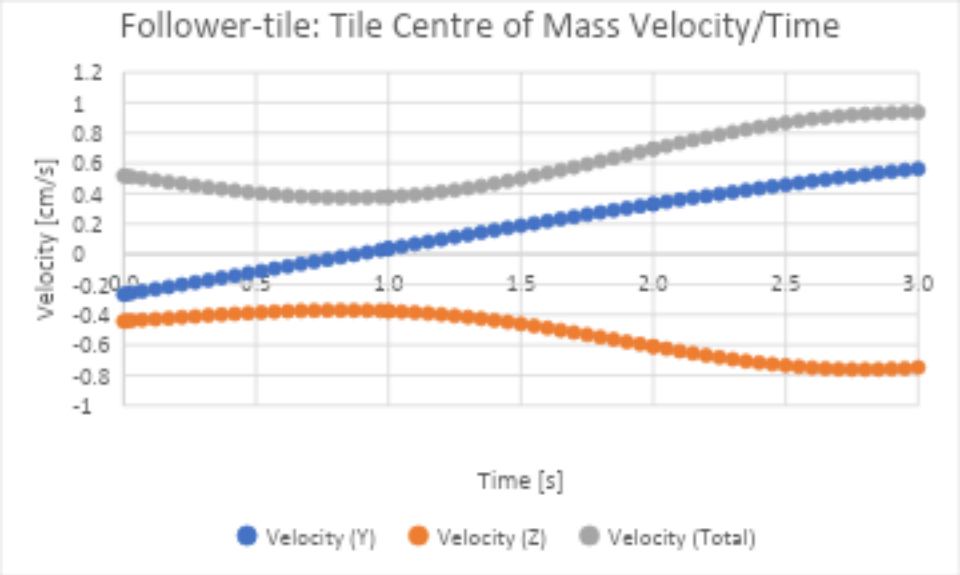

Figure 9

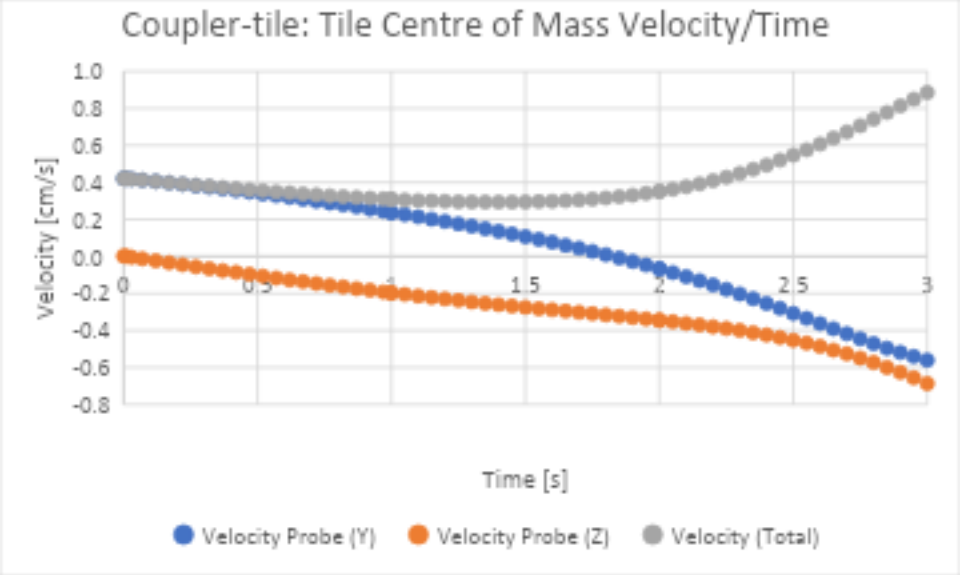

Figure 10

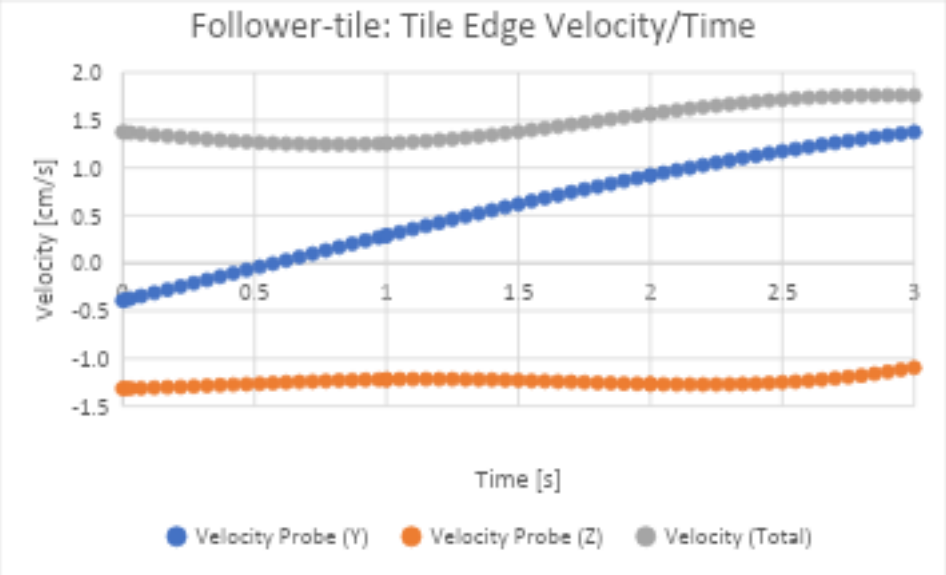

Figure 11

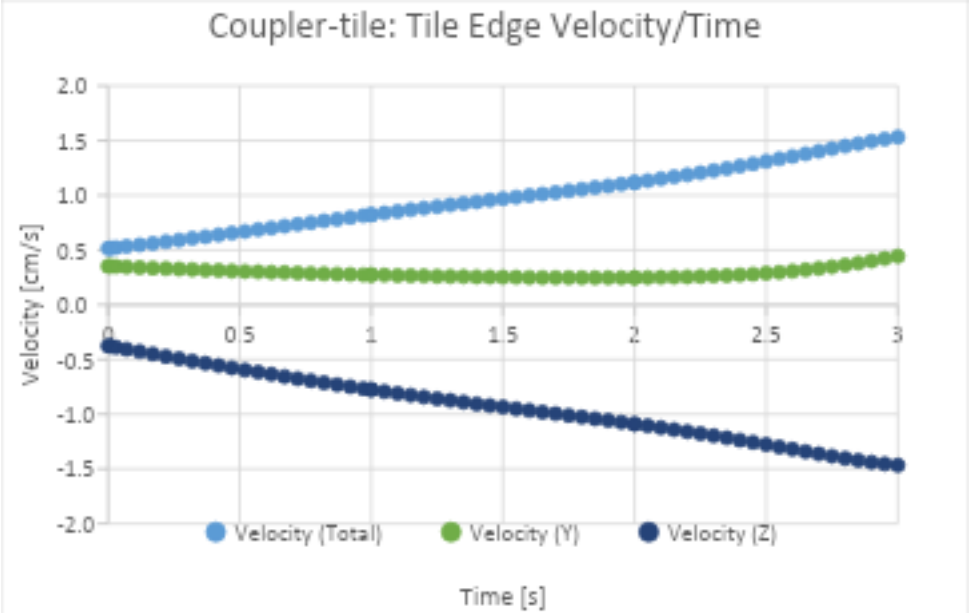

Figure 12

The follower-tile's overall velocity is higher than the coupler-tile model's, the speed of its centre peaking at 3 s *(Figure 9)* while that of its edge peaks at 2.5 s *(Figure 11)*, having relative speeds of 0.95 cm/s and 1.75 cm/s respectively.

Though the centre of inertia of the coupler-tile does reach the same highest point of the follower-tile, its speed stays under 0.5 cm/s for more than half of the duration *(Figure 10)*. And its total edge speed also lacks behind by measuring 1.5 cm/s at its highest *(Figure 12)*.

Overall, smooth curves are observed and therefore velocities did not have any spikes or discontinuities for the 3 second duration.

c) Acceleration

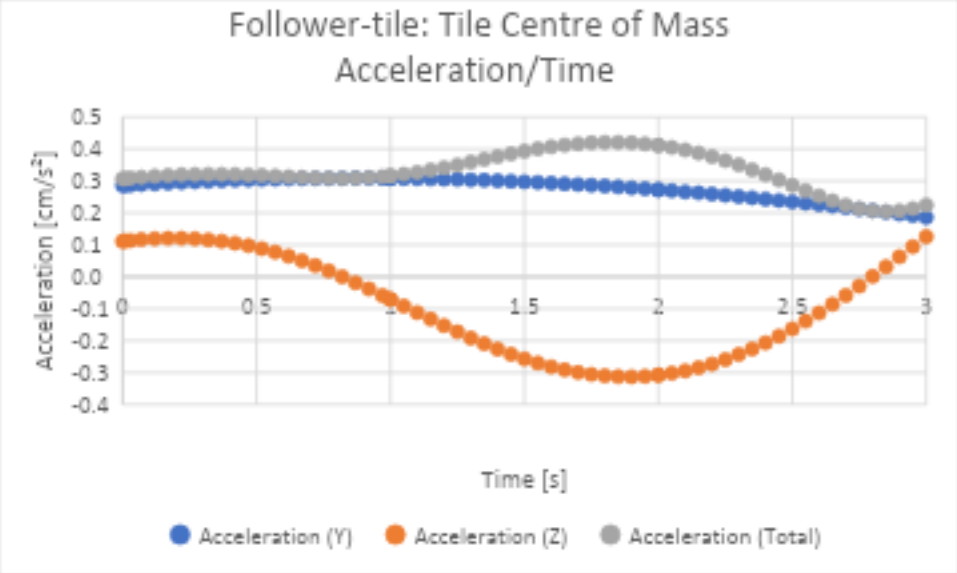

Figure 13

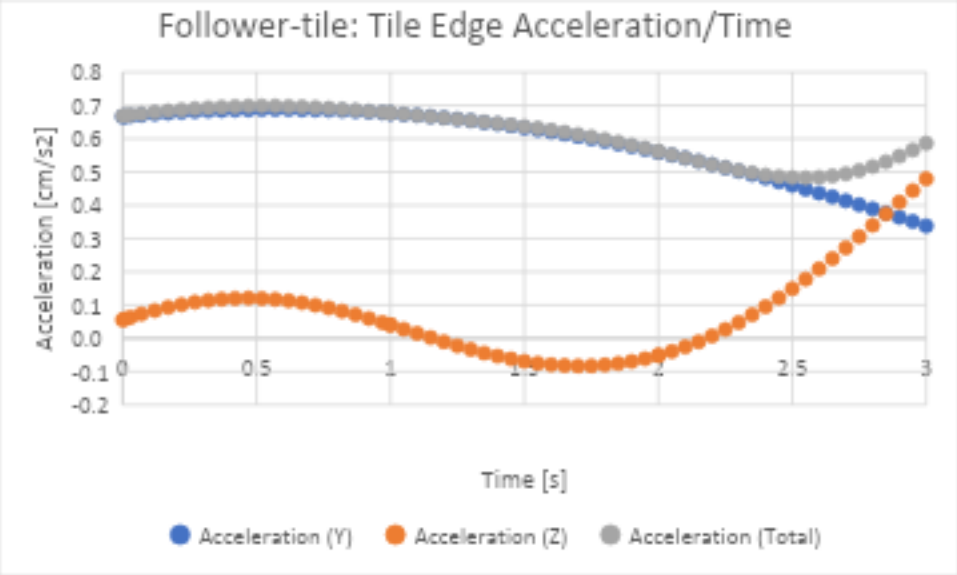

Figure 14

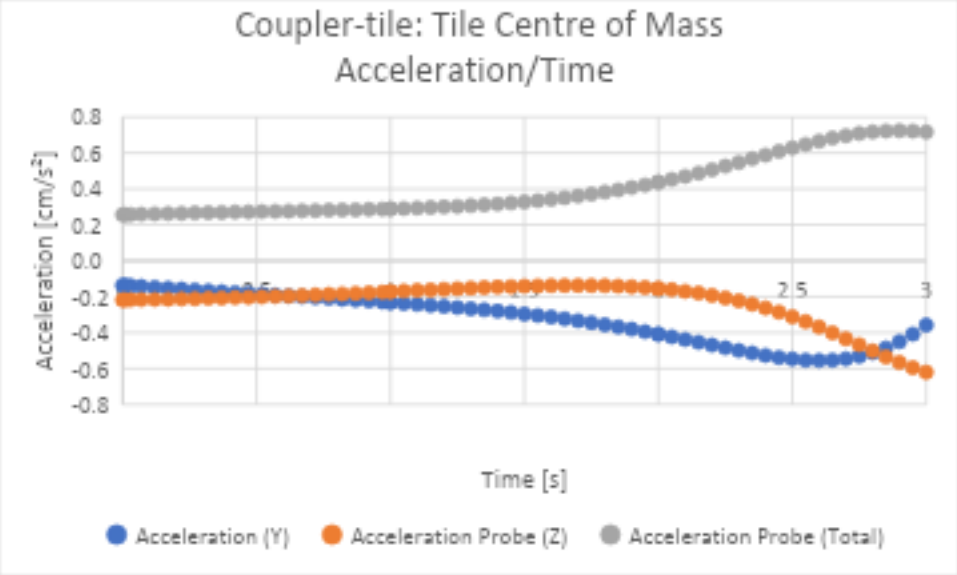

Figure 15

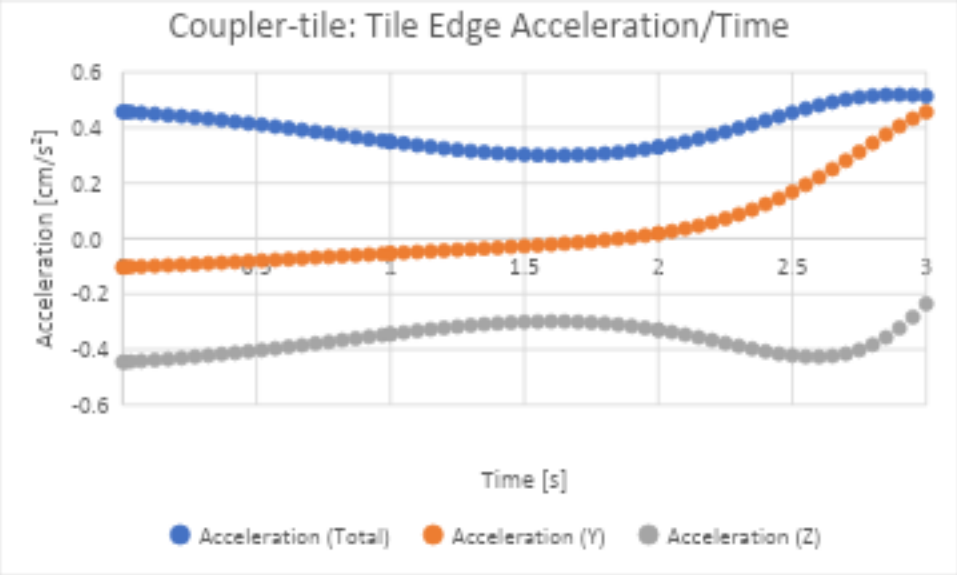

Figure 16

The total acceleration of the follower-tile's edge dips at 2.5 s, from 0.7 cm/s^2 to 0.5 cm/s^2, then rises when nearing 3 seconds, measuring 0.6 cm/s^2 *(Figure 14)*. This rise is because of the spike of acceleration at the z axis, but the inverse happens for the coupler-tile's edge. Its acceleration drops from 0.45 cm/s^2 to 0.3 cm/s^2 at 1.5 s. Afterwards, gaining acceleration on the y axis, its final and maximum acceleration measures 0.5 cm/s^2 *(Figure 16)*.

The centre of the follower-tile's acceleration shows similar trends in components to its edge, difference being the former's small magnitude. Starting at 0.3 cm/s^2, the graph stays level until an increase happens in 1 s, peaking at 1.8 s with a value of 0.45 cm/s^2, and later falling back down to 0.2 cm/s^2 *(Figure 13)*.

The total acceleration of the coupler-tile's centre mirrors its y-component across the x-axis, differing from that of the follower-tile, which mirrored its z-component. The initial acceleration of 0.25 cm/s^2 increases to 0.7 cm/s^2 at the end *(Figure 15)*.

d) Joint Forces

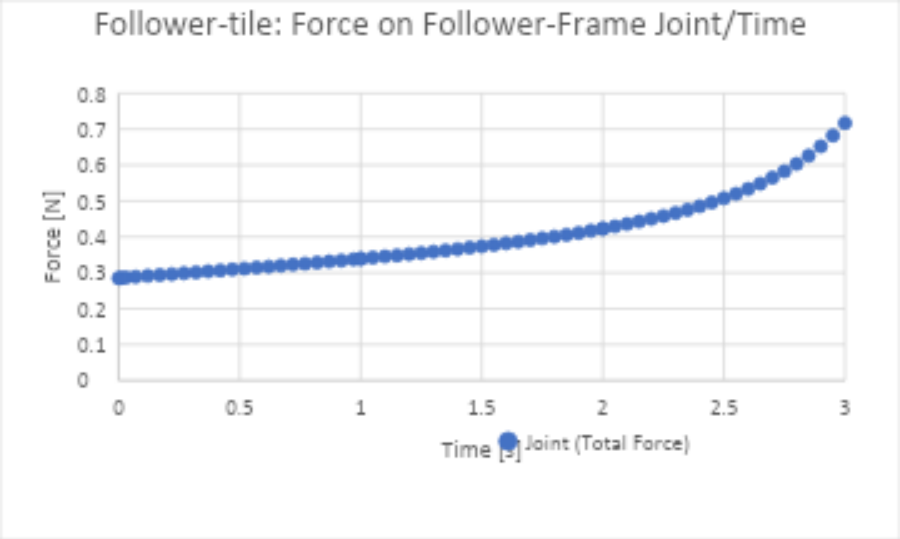

Figure 17

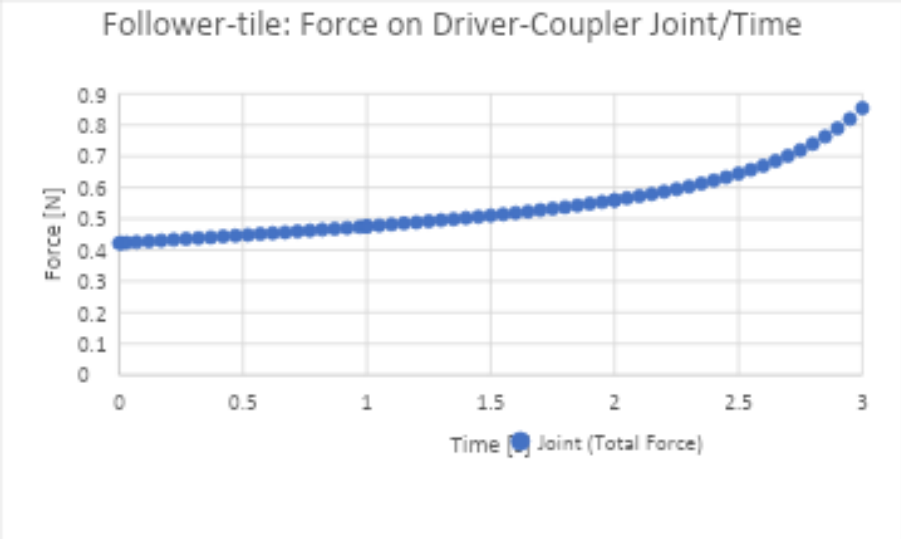

Figure 18

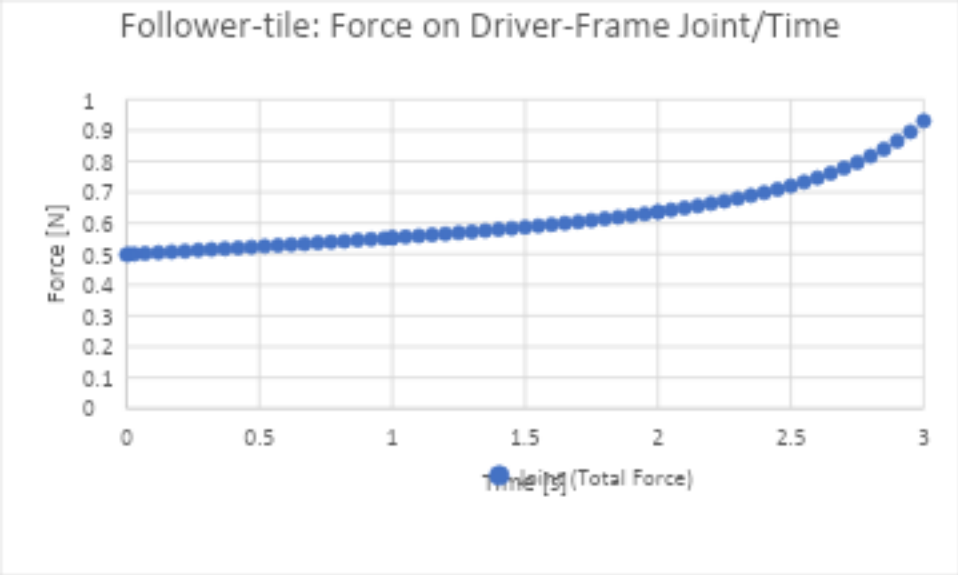

Figure 19

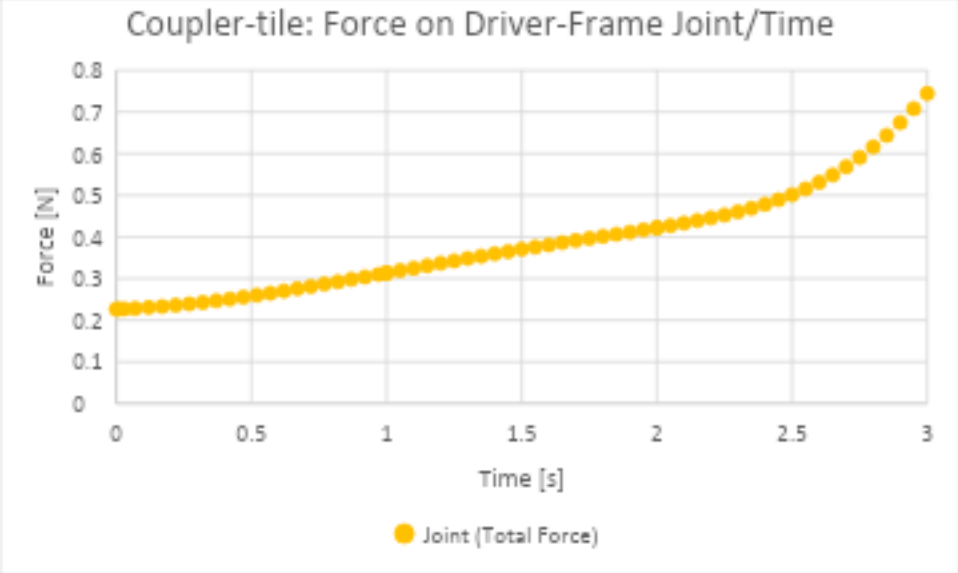

Figure 20

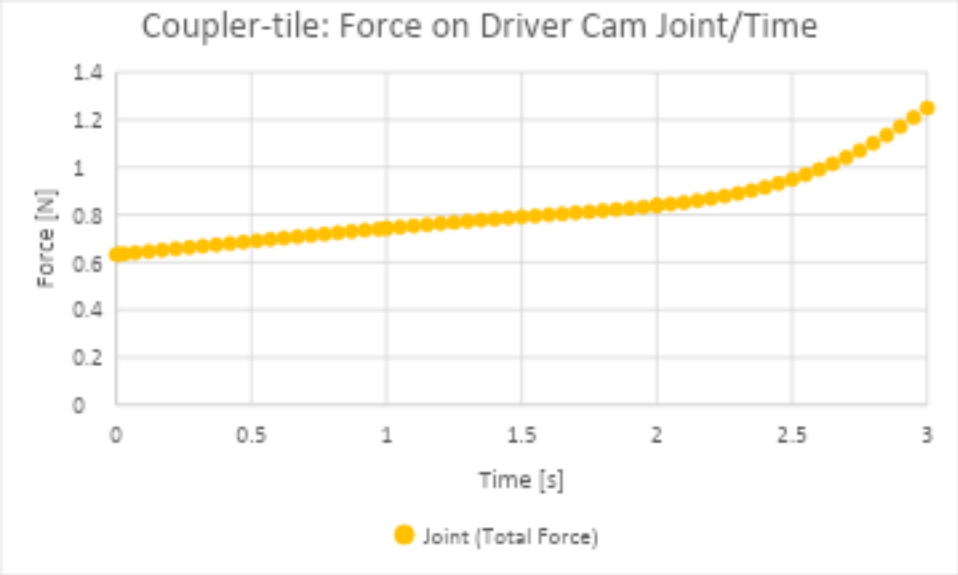

Figure 21

All of these joints show a consistent load increase without any sharp spikes while nearing the end of the tile's opening movement. The forces on the driver-coupler and the driver-frame joints of the follower-tile peak at around 0.9 N *(Figures 18 and 19)*, both increasing by 0.4 N. The follower-frame joint reaches 0.7 N with the same increase of 0.4 N *(Figure 15)*.

The driver-frame and the driver cam joints of the coupler-tile experience a force increase of 5.5 and 6 N, respectively *(Figures 20 and 21)*. While the maximum force on the driver frame is 0.75 N at 3 s, the force on the driver cam joint measures a maximum of 1.2 N, the highest of the gradual and constant increasing forces on the joints.

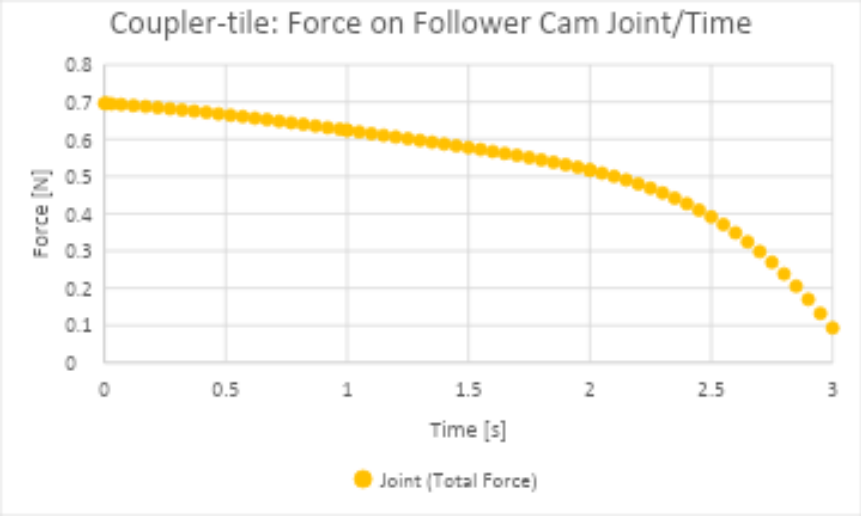

Figure 22

Contrarily, the follower cam joint is subjected to 0.7 N at the initial position; the force then smoothly lessening to 0.1 N *(Figure 22)*.

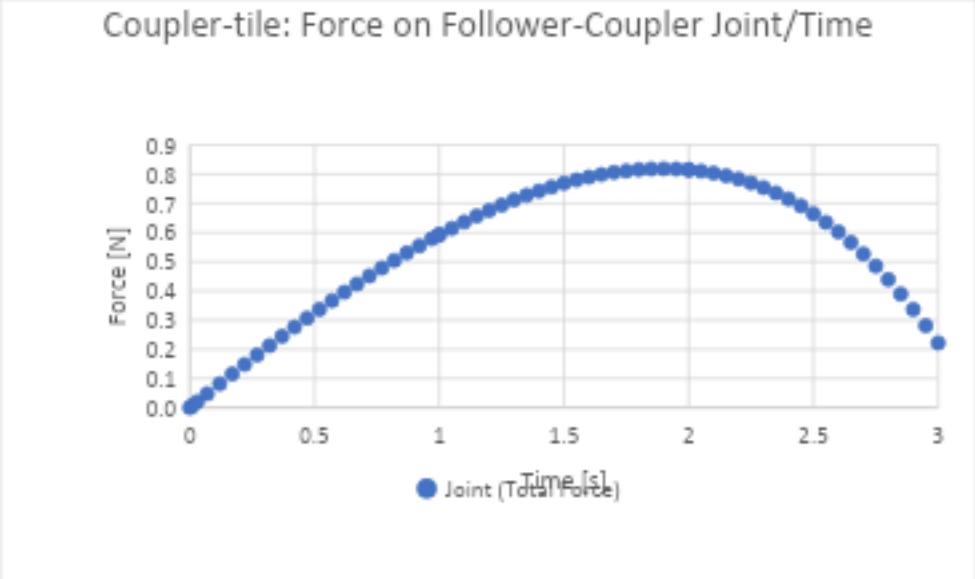

Figure 23

The force on the follower-coupler joint increases to 0.8 N from 0 N in the first 2 s, then declining to 0.2 N during the dwelling period of the cam *(Figure 23)*.

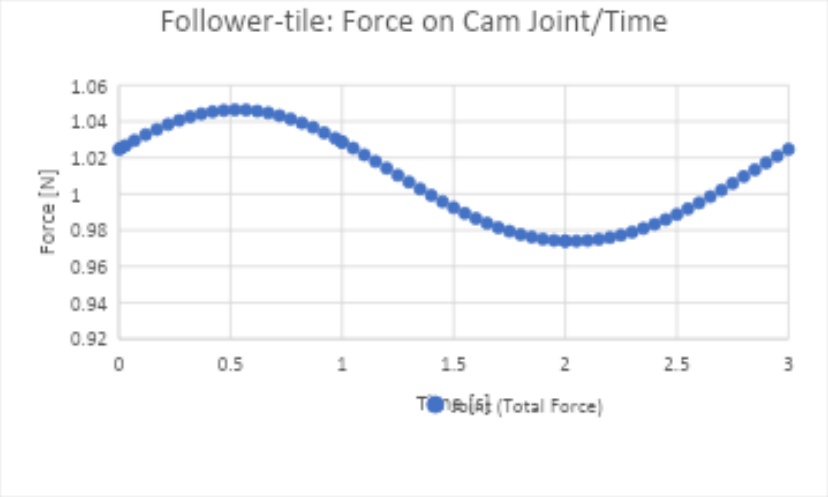

Figure 24

The periodic nature of a cam is apparent on the cam of the follower-tile, and the force decreases whenever the weight of the mechanisms aligns with the camshaft axis. The amplitude of this oscillation is 0.036 N with an equilibrium point of 1.01 N. Therefore, as seen on the graph, the maximum value of the force is 1.046 N while the minimum is 0.974 N *(Figure 24)*.

RESULTS

a) Position

From *Figure 5*, it can be observed that the centre of mass of the follower-tile experiences a total positional variation of approximately 1.5 cm. Despite the cam lifting the overall structure, the Z-component decreases, indicating that the centre of mass is lowered. This behaviour results from the edge of the tile lowering during motion, counteracting the rising motion. Meanwhile, the Y-position increases, which can be attributed to the tilting variations that occurs.

In comparison to the follower-tile, the coupler-tile *(Figure 6)* shows a smaller overall positional variation, measuring approximately 0.9 cm. Similar to the follower-tile, there is a decrease in the Z-component, meaning that even though the cam raises the structure, the combined tilting and lowering of the driver cause the centre of mass of the coupler tile to drop.

Additionally, the Y-position initially increases until around 1.8 seconds, after which it begins to decrease. This behaviour results from the followers angling away from the drivers briefly before the drivers' tilt motion pulls them back toward a more vertical position.

From *Figure 7*, which presents the edge position of the follower-tile, the Z-position decreases sharply, as this part experiences the greatest displacement to allow the opening of the tile. Meanwhile, the Y-position

also increases significantly, due to the swinging motion of the tile's edge nearing it to the frame. Overall, this results in a total positional variation of about 3 cm.

For the coupler tile's edge position *(Figure 8)*, a similar pattern is observed: the Z-component decreases noticeably, while the Y-component increases, again due to the more pronounced swinging motion experienced at the edge compared to the centre of mass. The total positional variation here is likewise around 3 cm.

b) Velocity

As observed in *Figure 9*, since the Z-component of the position decreases, the centre of mass of the follower-tile exhibits a negative velocity in the Z-direction, indicating a downward acceleration. The Y-component of the velocity is initially negative, caused by the handles of the follower. These protrusions that are necessary for the secure connection, and the extra length of the protrusion between the follower and the frame cause the centre of mass to deviate slightly toward the couplers at the beginning of the motion. After this effect subsides, the velocity increases until reaching 0.5 cm/s.

For the coupler tile's centre of mass *(Figure 10)*, the Z-component of velocity is negative, primarily due to the tile lowering caused by its tilt, which partially cancels out the follower cam's lift, and also because of the driver cam lowering a side of the structure. The Y-component of velocity initially starts positive but eventually turns negative. This behaviour arises from the follower's small outward tilt, which creates a positive Y-velocity, and then as the driver pulls the tile and creates the tilt, the follower becomes vertical once more. Thus, the centre of mass moves left, producing a negative Y-velocity.

Examining the edge of the follower-tile *(Figure 11)*, the Z-velocity remains negative, while the Y-velocity increases significantly due to the larger distance travelled by the edge, resulting in an almost constant velocity with minor oscillations.

For the coupler tile's edge velocity *(Figure 12)*, the Z-component remains negative, also reflecting the downward motion at the tile's opening. Along the Y axis, the motion of the edge could be likened to the reflection of a circular movement around the coupler-follower joint. This would mean that during the first phases of the movement, the velocity should be low, accelerating towards the end. Yet this is not the case, the Y-component staying nearly constant. This is due to the tilt the followers experience, being tilted outward initially, increasing speed. Later, they swing back toward the drivers and become vertical once again, pushing the edge towards the left. The culmination of these movements results in an almost constant velocity. In the end, the total velocity experiences constant acceleration.

c) Acceleration

The centre of mass *(Figure 13)* and edge *(Figure 14)* of the follower-tile show very similar trends because of their alignment. However, the edge experiences larger displacements, resulting in higher acceleration values overall. Interestingly, the lowest acceleration of the Z-component of the centre of mass is lower than that of the edge. This can be attributed to the fact that while the edge experiences a greater downward velocity, the effects of the raise by the cam are more pronounced at the centre because of this.

Therefore, after the speed caused by the cam subsides nearing the middle, the centre experiences a greater acceleration.

For the coupler tile, the acceleration increases toward the end of the motion. This occurs because the driver completes its motion, causing the leaned-back frame to realign itself with the z-axis, resulting in the largest movement at the end. The centre of mass *(Figure 15)* experiences an acceleration toward the ground due to the tilt and the realignment of the followers, and an acceleration toward the left as the realignment pushes the tile.

However, the Y-component of acceleration of its edge increases *(Figure 16)*. This is because of the motion of the topmost part of the tile toward the left, causing the edge to move to the right. The Z-component is negative, as the edge also accelerates towards the ground.

d) Joint Forces

For the follower-tile, the forces on the follower-frame, driver-coupler, and driver-frame increase as the tile moves toward a more vertical position *(Figures 17, 18, and 19)*. This increase occurs because the acceleration of the tile toward the ground amplifies the load that the joints must support.

For the coupler-tile, the driver-frame *(Figure 20)* joint sees an increase in load because the driver and driver frame move out of alignment, which raises torque and load bearing. Additionally, the driver cam joint force *(Figure 21)* rises because, initially, the cam shaft, driver, driver frame, and cam centre are aligned. As the simulation progresses and the cam lowers the tile, the cam centre goes out of line, which increases the torque on the joint. One other reason is that the cam's motion causes more movement along the Z axis as the simulation nears its end and the cam centre-cam line becomes perpendicular with driver frame base-cam line.

The force on the follower cam joint *(Figure 22)* decreases compared to its great initial value. This is because at the initial position, the cam centre, cam shaft, and follower frame are at the position furthest from alignment. As the cam lifts the tile, these components become increasingly more aligned, which reduces torque and therefore lowers the force.

For the follower-coupler joint *(Figure 23)*, the slight backward lean of the follower causes it to go out of alignment with its centre, generating torque. Much of the tile's load is carried by this joint because the opposite side of the tile lowers. As the motion progresses, the backward lean is corrected, reducing the force, though it does not drop entirely, since the coupler-driver joint still carries a smaller portion of the load.

Finally, regarding the follower-tile's cam joint *(Figure 24)*, the force oscillates. This occurs because as the cam centre moves out of line with the cam shaft and frame, the force increases, and as alignment improves, the force decreases with the reduction in torque. At the end of the 3 seconds, during the dwelling period, the force rises again as the cam centre shifts out of line, requiring applied force to maintain the current position.

DISCUSSION

Based on the quantitative data gathered, and the following interpretations, several observations can be made. The lack of any spikes or reversals in the position graphs *(Figures 3-6)* indicate the designs' efficiency. The retrieved results are in accordance with the intended motions, and therefore the modelling aspect is considered a success.

The velocity graphs *(Figures 9-12)* consolidate that the designs showed proper behaviour. While lack of spikes and conflicting data indicate reliability, the high velocities at the end of the simulations point to necessary improvements. The assignment of constant angular velocities was done to simplify the simulations' load. However, this caused unnecessary speed to remain at the end of the motion, which will lead to an impact between the mechanical parts. The crash will decrease the longevity and lower the efficiency.

This can further be seen from the acceleration graphs *(Figures 13-16)*. As mentioned before, because the closing of the tiles will mirror that of the opening, the remaining acceleration will either result in the aforementioned impact or the relatively great requirements of force to counteract the final accelerations.

Although this simplification of using a constant angular velocity rather than realistic acceleration and deceleration profiles, the resulting joint load graphs remained smooth and free of spikes. This consistency and the well-coordinated movements shown in the position graphs suggest that, with correctly applied motion parameters, the mechanisms could operate without collisions or energy waste. However, even at this stage, the mechanisms take no longer than a human's capture move, greatly improving upon the existing capture systems of chess automation mechanisms.

Furthermore, the differing designs could have different uses. The simplicity of the follower-tile design would greatly reduce 3D printing or manufacturing costs. Moreover, the greater amount of tilt of this design would indicate to higher reliability. The constantly high and oscillating force on its cam joint and the increased load on the driver-coupler joint could limit its longevity, requiring more replacements. However, it is cheaper and more compact in return.

The more complex and larger coupler-tile design would be harder to produce, and the intricate parts would render this harder to replace. However, this design could be modified to a greater extent as the driver and follower frames have many possibilities of improvements and changes.

In addition to the mentioned improvements of better and more realistic motion definitions and design changes, the employment of different mechanical linkages could be explored.

CONCLUSION

The purpose of this study was to offer new capture-dedicated mechanisms to chess automation systems with the aim of lessening capture move durations. This was achieved by the creation of two designs that would fit under each tile, capable of opening to let the captured piece fall into the chessboard to be collected at the end of the match. The two designs were analysed, comparing positional, velocity, acceleration, and joint force graphs on key points. The follower-tile design was concluded to have greater mobility while possessing fewer parts. The coupler-tile design was concluded to have improved longevity compared to the follower-tile, having lower overall forces on its joints. However, the increased complexity was a drawback. Overall, both designs achieved the intended tilt, improving upon the capture time of existing designs.

These new models could be better analysed by running more accurate simulations, better regulating the angular velocities of joints. A complete chessboard could also be simulated in order to better contextualise the findings. The omitted frictions and mechanism materials could be taken into consideration to simulate the products with higher accuracy. Lastly, different cam profiles could be utilised to get a specific rise and fall sequence.

REFERENCES

[1] F. Y. Ómarsdóttir, R. B. Ólafsson, and J. T. Foley, "The Axiomatic Design of Chessmate: A Chess-playing Robot," in *Procedia CIRP*, Elsevier B.V., 2016, pp. 231–236. doi: 10.1016/j.procir.2016.07.002.

[2] T. D. Phuc and B. C. Son, "Development of an autonomous chess robot system using computer vision and deep learning," *Results in Engineering*, vol. 25, Mar. 2025, doi: 10.1016/j.rineng.2025.104091.

[3] C. Jariyavajee, A. Visavakitcharoen, P. Sirimaha, B. Sirinaovakul, and J. Polvichai, *A Practical Interactive Chess Board with Automatic Movement Control*. [IEEE], 2018.

[4] S. Sarker, "Wizard Chess: An Autonomous Chess Playing Robot."

[5] S. R. Kashef, S. Amini, and A. Akbarzadeh, "Robotic hand: A review on linkage-driven finger mechanisms of prosthetic hands and evaluation of the performance criteria," Mar. 01, 2020, *Elsevier Ltd*. doi: 10.1016/j.mechmachtheory.2019.103677.

[6] Q. T. Truong, Q. V. Nguyen, H. C. Park, D. Y. Byun, and N. S. Goo, "Modification of a four-bar linkage system for a higher optimal flapping frequency," *J Intell Mater Syst Struct*, vol. 22, no. 1, pp. 59–66, Jan. 2011, doi: 10.1177/1045389X10392611.

[7] M. R. Mali, P. D. Maskar, S. H. Gawande, and J. S. Bagi, "Design Optimization of Cam & Follower Mechanism of an Internal Combustion Engine for Improving the Engine Efficiency," *Modern Mechanical Engineering*, vol. 02, no. 03, pp. 114–119, 2012, doi: 10.4236/mme.2012.23014.

[8] R. D. V. Prasad, K. Satyanarayana, Ch. Maheswara Rao, and M. S. S. Srinivas Rao, "Analysis of Cam and Follower Mechanism to Reduce Jerk and Induced Stresses," *Journal of Recent Trends in Mechanics*, vol. 5, no. 3, pp. 8–17, Dec. 2020, doi: 10.46610/jortm.2020.v05i03.002.